

Chinook Helicopter and Slung Load Coupled Body Dynamic Simulation

KR Reddy, TT Truong, KJ Bourne, RA Stuckey and N Blacker

Defence Science and Technology Organisation, Department of Defence
506 Lorimer Street, Fishermans Bend, VIC 3207, Australia

Keywords: Slung load simulation, parametric study, helicopters, coupled body dynamics, Chinook, CH-47D

ABSTRACT

The aim of this work is to develop a comprehensive simulation package that can be used to define the safe operational limits of an Australian Army CH-47D Chinook when carrying single or multiple slung loads. This paper presents the work that has been carried out to date, in particular the development of a simple helicopter slung-load model for simulation and analysis of the system dynamics. A range of numerical results are presented in which simulation is used to study problems encountered by the Australian Army during CH-47D slung load operations. Case studies presented include the following loads; a water tank, a Medium Maintenance Shelter (MMS), a Rigid Inflatable Boat (RIB) and a Tiger Armed Reconnaissance Helicopter (ARH). The simulation model is also used to identify parameters of importance and the associated effects on the dynamic stability of the coupled body system. The parameters examined are helicopter speed, load mass and its centre of gravity (cg) location, pilot control inputs, rigging configurations, load geometry, and load aerodynamic properties.

1. INTRODUCTION

In support of regular Army and Special Air Service (SAS) operations, the CH-47D regularly carries external loads, as seen in Fig. 1. The safety and operational flight envelope of helicopters carrying externally slung loads is limited and sometimes seriously hindered by stability and control problems. Several incidences have been reported by the Australian Army in which possible aerodynamic excitation or dynamic instability of the slung load has resulted in a forced premature release of the load.

Previously, there were no simulation tools that could be used successfully to predict the flight conditions under which a particular load becomes unstable. The safe operating envelope for slung loads is established through flight tests over a range of increasing airspeeds. This is a

very costly exercise and is not without some risk. Consequently, the Australian Defence Science and Technology Organisation (DSTO) is developing a comprehensive simulation program to assist in defining the operational limits of various Australian Defence Force (ADF) helicopters when carrying slung loads. A central part of the program has entailed the development of a detailed helicopter slung load model [1] based on research from the National Aeronautics and Space Administration (NASA) Ames Research Center [2].

This is a highly complex dynamic system requiring detailed dynamic and aerodynamic representations of both the helicopter and the load. Initially, the primary goal of this work was to define the operational limits of the Australian Army Chinook CH-47D when carrying multiple, mixed density slung-loads.

However, the focus has since shifted to the study of the dynamics of the CH-47D with single, aerodynamically active, slung loads, that is, loads with aerodynamic characteristics that typically have a low mass density and some lifting behaviour.

One of the driving forces behind the shift in focus was an incident that occurred during an Australian Army flight trial where, during the flight, an underslung RIB came into contact with the Chinook fuselage. This was not the first instance where instability had forced the load to be ditched, however prior to the RIB incident no load had ever come so close to causing a catastrophic outcome.



Figure 1 Chinook carrying single and multiple loads [3]

Another driver behind the shift in focus was a recent requirement to investigate the carriage and aerodynamic behaviour of an ARH Tiger as a slung load. The aerodynamic nature of the load has led to a number of challenges during model development. In particular, the accurate estimation of aerodynamic force and moment characteristics of the load, and the avoidance of numerical convergence problems required significant attention.

The overarching goal of this research is to build a capability that will provide an initial estimate of the dynamic behaviour and stability of any particular helicopter slung-load configuration prior to flight testing.

In this paper, a broad overview of the model development and its implementation in MATLAB is first

presented. The successful outcome of this simulation relies on three elements; a flight dynamic model of the helicopter, a good dynamic and aerodynamic representation of the load, and an appropriate approximation of the rigging arrangement.

RotorGen, a flight dynamic model used to represent the Chinook helicopter, is discussed, followed by the methods used to estimate load aerodynamic characteristics. Aerodynamic and dynamic load information is not often readily available. The operator is then compelled to develop appropriate data sets based on experience and where applicable the use of simple body shapes such as flat plates, cones and cylinders. A Computational Fluid Dynamics (CFD) program that has been initiated to calculate aerodynamic properties of the load will also be discussed, and initial results presented [4].

Numerical results in which simulation is used to study some practical Australian Army operational problems are then presented. These include a CH-47D carrying a water tank, a MMS, a RIB and an ARH Tiger. The simulation model is also used extensively to identify important parameters and the effect of these on dynamic stability of the coupled body system. Some of the parameters used in sensitivity studies include helicopter speed, load mass and its cg location, pilot control inputs, rigging configurations, load geometry and load aerodynamic properties.

In the final section of the paper, some concluding remarks are drawn and proposals for further work are made.

2. MODEL DEVELOPMENT

Helicopter slung-load systems fall into a class of multi-body systems approximated by two or more rigid

bodies connected by links. The links can be considered either elastic or inelastic, although the rigid-body assumption excludes any helicopter or load elastic modes. Typically, the system is characterised by the configuration geometry, mass, inertia, and aerodynamic behaviour of both helicopter and load, as well as the elastic properties of the links.

In general terms, the system of interest consists of a single helicopter supporting one or more loads by means of some suspension. The model is comprised of n rigid bodies, with m straight-line links supporting a single force in the direction of the link. If the links are modelled as inelastic, $c \leq m$ constraints are imposed on the motion of the bodies and the system has $d = n*6 - c$ degrees-of-freedom (dof). If the links are modelled as elastic, there are $n*6$ dof.

A number of simplifying assumptions have been made in the model. These include the exclusion of cable mass, cable aerodynamics and rotor-downwash effects. To account for a lack of downwash effects, the program is only used to study cases where the helicopter's forward speed exceeds 40 knots. Despite these limitations, the system has proven adequate for simulation studies in which the low-frequency behaviour is of primary interest and the helicopter is initially trimmed in forward flight.

The simulation model used is based on the helicopter slung-load system introduced by Cicolani, *et al* [2]. In this formulation, the general system equations of motion are obtained from the Newton-Euler equations in terms of generalised coordinates and velocities. Details of the model development can be found in Stuckey [1, 5]. Aside from the core helicopter model, all code development has been performed in the MATLAB [6] numerical computing environment.

The Helicopter Slung-Load Simulation program HSLSIM consists of several modules, written in the MATLAB language. These include the main script, an optimisation routine, a differential equation solution, an integration function, a flight-dynamic model, and various output and replay functions. There is also a graphical user interface for simplified control of the primary program functions. Alternatively, the simulation can be run through a main script, which generates the control inputs, configures the helicopter-load system properties (geometric and inertial), sets the initial system state, and then executes the trim and integration functions.

For successful simulation two components, the helicopter and the slung load, need to be modelled in detail. The flight dynamic model, RotorGen, is used to model the helicopter aerodynamics, dynamics and control system. A range of methods are employed to estimate load aerodynamic properties. The following section presents a broad review of helicopter and load representations as used in the study.

3. HELICOPTER MODELS AND LOAD AERODYNAMICS

RotorGen was developed by Heffley [7] for the US Army Aeroflightdynamics Directorate under NASA contract to Hoh Aeronautics, Inc. It is described as a minimal-complexity generic rotorcraft model intended for manned simulation of large military helicopters and, in particular, the CH-47D Chinook tandem rotor helicopter. The rotor inflow model is based on Glauert's representation of thrust, with the orientation (incidence) of the tip path plane defined by a set of flapping equations. The body forces are based on a quadratic fluid-dynamics formulation, applicable to low-speed flight. RotorGen is a combination of two existing flight models: the Extended

Stability Derivative (ESD) model developed for NASA, and the RotorGen thrust model developed for the US Army.

As such, the RotorGen model has a modular structure, which combines several features of the original ESD model. These include a primary Flight Control System (FCS), rotor and body forces, ground effects, and a Stability and Control Augmentation System (SCAS). The core helicopter dynamics and control models were integrated into the slung load simulation package HSLSIM developed at DSTO. The inputs to RotorGen consist of the current flight state (orientation, rates, and altitude) and the control inputs. The outputs consist of the resultant forces and moments from both main rotors and the fuselage. In addition to interfacing and initialisation code, a set of trim routines was developed so that the simulation could be flown from an equilibrium state.

Loads requiring transportation typically tend to be bluff bodies operating in subsonic flows with high angle of flow incidence. Aerodynamic data for such bodies is often unavailable.

For the incident investigation involving the RIB, several generic aerodynamic models were combined to represent the RIB. These included a Conex container and a cylinder with a rounded end. The aerodynamic data for the Conex container was taken from Ronen [8] which was itself a compilation of several other aerodynamic models obtained from experiment. The aerodynamic behaviour of the cylinder was taken from Hoerner [9] and ESDU [10] in the form of analytical equations dependent on the free-stream Reynolds number and the angle of incidence. Since the RIB was to be carried as an external load and would have the freedom to swing through large angles in flight, the model also needed to

cover the entire angle-of-attack and sideslip range from -180° to 180° . In situations where a model must be generated from composite shapes, clear understanding of the effect of various aerodynamic parameters on load oscillations is advantageous. In the following section, results of such a study are presented.

Generating aerodynamic characteristics of a bluff body by combining a range of simple body shapes can be quite challenging. To improve the speed at which complex shapes can be modelled aerodynamically, a CFD program has been initiated. Some results of this research are presented in the next section.

4. NUMERICAL RESULTS AND DISCUSSION

In this section a range of numerical results are presented. In each case the simulation model is used to identify the effect of variation in key parameters on dynamic stability of the helicopter slung-load system.

It is important to note that this research is still continuing and the results presented in this paper, though comprehensive, may not be complete. Hence the results and the concluding remarks should not be viewed as final statements.

4.1 Effect of Speed and Load Mass

An Army water tank simulation model was used to demonstrate the effects of speed and load mass variations. Figure 2 shows the water tank, which is $8 \times 6.5 \times 3.8 \text{ ft}^3$. The simulation was performed over a range of airspeeds and load mass values. Results are shown in Fig. 3 and displayed in terms of the maximum deviation of the load cg position with respect to its trim position.



Figure 2 Australian Army water tank

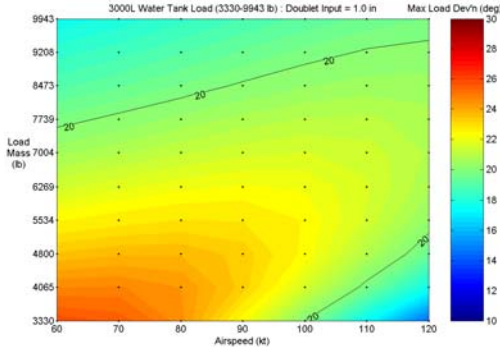


Figure 3 Maximum load position deviation as a function of airspeed and load mass

Observing the resulting maximum load position deviation from variation in both airspeed and load mass, quite a distinct trend is evident. For relatively low masses and low speeds (below 5500 lbs and 90 kt) load position deviation is highest.

For this test case, load position deviation decreases with increases in airspeed and increases in the load mass. Load stability is clearly a function of both airspeed and mass, with the most critical cases being those with light loads and low airspeeds.

4.2 Effect of Speed, Load cg and Pilot Control Inputs

To investigate the effects of variation in load cg position and pilot control inputs, an MMS simulation model was chosen. The medium maintenance shelter is $13 \times 8 \times 7$ ft³ and weighs 4000 lbs. To achieve a controlled initial load disturbance, a 0.5 inch lateral manoeuvre was executed.

For further details of the control input profiles, see Stuckey [1].

The load was suspended by cables that provided a 20 ft separation between helicopter cg and load cg. The altitude of the helicopter cg was set at 200 ft. The slings were in a tandem configuration, as shown in Fig. 4.



Figure 4 CH-47D carrying an MMS

The combination of the load's cg position and its airspeed has a significant effect on load stability. From Fig. 5 it can be seen that as the cg location is moved further aft, the load becomes increasingly unstable. The higher the airspeed, the lower the tolerance to aft cg positions if the load is to remain stable. For example, at an airspeed of 60 knots the load becomes unstable once the cg is moved more than 3 ft behind the centre of the load. At an airspeed of 90 knots, a cg position aft of centreline at any distance results in significantly increased maximum load position deviation.

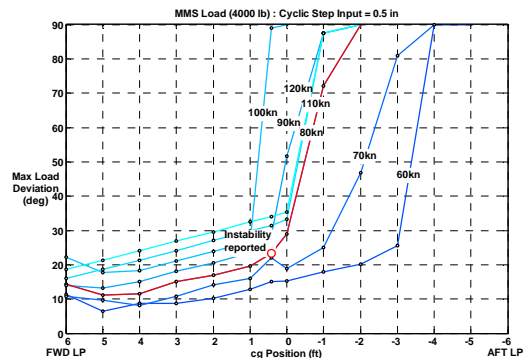


Figure 5 Effect of varying cg on maximum load position deviations

When the effect of pilot control inputs is considered with respect to the load's cg position, Fig. 6 shows that the greater the control input magnitude, the greater the maximum load position deviation. Figure 6 also shows that increasing airspeed increases the maximum load position deviation.

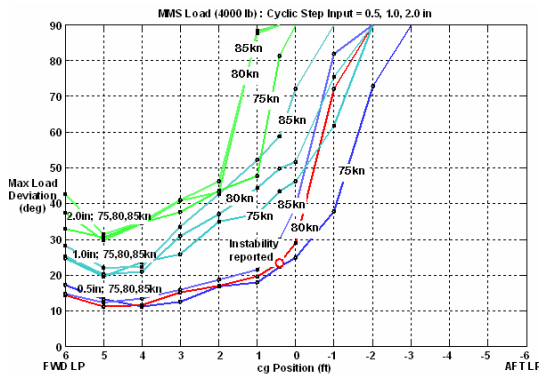


Figure 6 Effect of varying pilot control inputs on maximum load position deviations

For this example, maximum load position deviation is dependent on both airspeed and the magnitude of the pilot control inputs. The general trend indicates that increasing either of these variables increases the sensitivity to aft cg positions, resulting in an earlier onset of load instability.

The instability reported in Figs 5 and 6 was observed by the ADF Air Movements Training and Development Unit (AMTDU) during flight trials.

4.3 Effect of Load Orientation

In 1998 the Australian Army conducted a slung load flight trial for the Rigid Inflatable Boat with the CH-47D. The load had previously been cleared for carriage in the bow-aft orientation, however a new request required the RIB be transported in the bow-forward position. The difference between configurations is shown in Fig. 7.

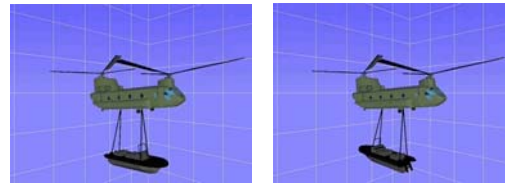


Figure 7 Bow-forward (left) and bow-aft (right) RIB orientation

At low speeds the RIB exhibited no unusual behaviour. Flight testing continued and forward speed was increased. It was during a transitional manoeuvre at high speed that the RIB made contact with the CH-47D fuselage. The sudden excitation, caused by aerodynamic instability, was not anticipated given no significant movement had been detected by loadmasters up to that point, and no equivalent excitation occurred for the bow-aft configuration.

To simulate the effect of varying load geometry, the RIB aerodynamic model was constructed as previously mentioned. The same sling configuration used during the flight test was implemented in the simulation, and a lateral manoeuvre used to represent the pilot input responsible for the load disturbance.

It was found that whilst the bow-aft RIB configuration remained stable at all tested airspeeds, the bow-forward orientation became violently unstable.

Fig. 8 shows the movement of the RIB cg beneath the CH-47D in terms of lateral and longitudinal displacement. As can be seen, the displacement of the bow-forward RIB far exceeds that of the bow-aft configuration.

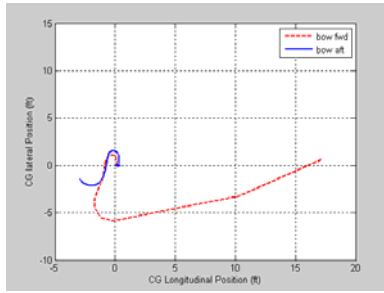


Figure 8 RIB load oscillation

4.4 Effect of Rigging Configuration

To test the effects of sling rigging configuration, the movement of an arbitrary box load was investigated. The box was given dimensions $15 \times 10 \times 10$ ft³ and a mass of 5000 lbs. The model was tested at an airspeed of 80 kt, and a lateral pilot control input of 1.5 inches. The actual cable length for each sling configuration varied to ensure a separation between load and helicopter of 25 ft. Each sling configuration is shown in Fig. 9.

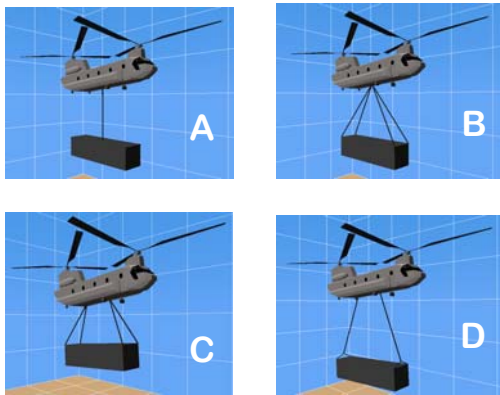


Figure 9 Rigging configuration; A single point, B multiple point, C tandem and D bifilar

Figure 10 shows that the load oscillation characteristics are unique to each sling configuration. There is also a clear difference between the sling configurations which utilise only a single connection point underneath the helicopter (single and multiple) and those which require two connection points (tandem and bifilar).

In this study the tandem and bifilar sling configurations yield higher load position deviation. This can be attributed to the fact that the load's movement is more tightly coupled to that of the aircraft. For both multiple and single sling configurations, the load is less effected by helicopter movement (although this does not necessarily mean that the load is more stable). The single and multiple sling configurations exhibit similar oscillatory motion, however the mutiple configuration shows more longitudinal displacement.

It is worth noting that any rotation of the load, which may be more pronounced for the single and multiple sling configurations, cannot be identified from Fig. 10. This information can be obtained from HSLSIM, but is not included in this analysis.

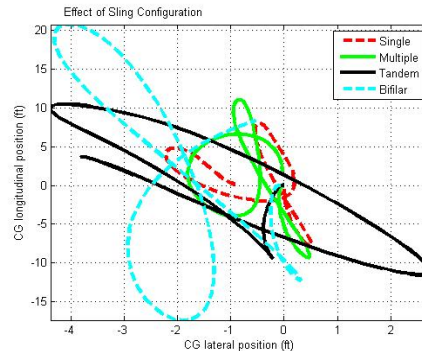


Figure 10 Effect of rigging configuration on maximum load oscillations

The bifilar and tandem configurations show some similarities between them, but not the degree of likeness seen between the single and multiple sling configurations. Of all configurations, the tandem slings result in the greatest lateral load displacement, however the bifilar configuration exhibits the largest longitudinal load displacement as well as the greatest overall maximum load position deviation.

4.5 Effect of Load Aerodynamics

Aerodynamic data for ARH Tiger fuselage is currently unavailable. In order to conduct a representative parametric study of the effect of variation in aerodynamic coefficients, Black Hawk aerodynamic data was used in place of ARH fuselage data. Although there are significant geometric differences between these aircraft types, it was deemed a reasonable substitution when compared to the alternative of using box aerodynamics. In place of an accurate geometric model, an equivalent load size of $36 \times 15 \times 16 \text{ ft}^3$ was used for the ARH and a weight of 10000 lbs was assumed, representative of the dry weight of an ARH Tiger.

Plan views of the load oscillations for a selection of load aerodynamic parameters are shown in Figs 11 to 14.

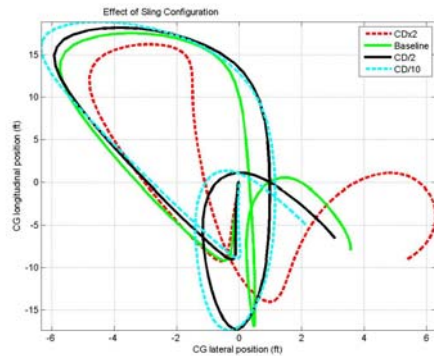


Figure 11 Effect of drag (CD) variation

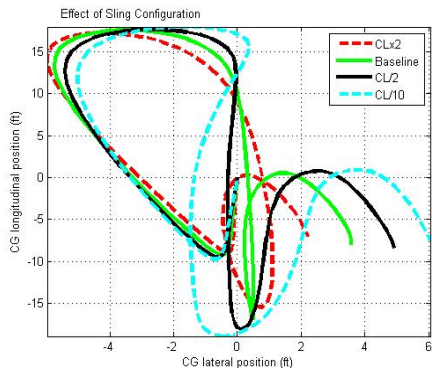


Figure 12 Effect of lift (CL) variation

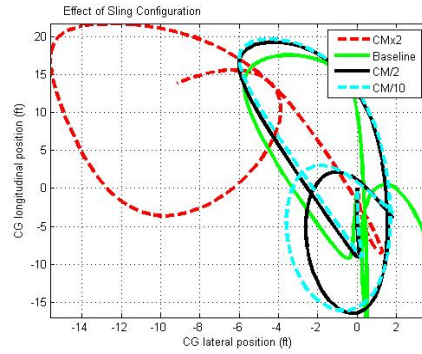


Figure 13 Effect of pitching moment (CM) variation

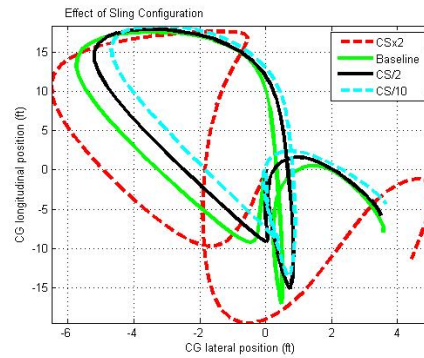


Figure 14 Effect of side force (CS) variation

Variation in the drag coefficient (CD) yielded intuitive results. As CD was increased, the load position deviation decreased. From Fig. 11 it can be seen that broad trends are similar for all CD.

Fig. 12 shows the effects of variation in the lift coefficient (CL). For most results, increasing CL decreased overall load displacement. Although unexpected, this is most likely due to the fact that whilst in a forward flight trim position, insufficient airflow is able to gather underneath the load to excite the increased CL. Increasing CL does have the subtle effect of making the load more ‘buoyant’, and so its reaction to the helicopter’s motion is slightly slower. This slower reaction time appears to alter the rocking motion of the load, in this case reducing maximum load position deviation.

The results for variation in the pitching moment coefficient (CM) are shown in Fig. 13. Unlike the other coefficients tested, for most results, any change to CM from the baseline tended to result in an increase in the overall load position deviation. The increase in load displacement associated with decreasing CM was significantly lower than the increase seen when CM was increased. This behaviour could not easily be explained. Further examination of results found that the initial position of the load for the case of CMx2 was nose-up, an unexpected trim position. This gave way to significant load position deviation when the load became unbalanced and pitched nose-down, transitioning to comparatively excessive oscillatory behaviour. For the reduced CM values, the load trim positions had nose-down orientations, resulting in more moderate load displacement traces.

Variation in the side-force coefficient (CS), as seen in Fig. 14, indicated that an increase in CS increased load position deviation. The path of oscillation is similar for the baseline and reduced CS values. For the case of CSx2, the load position deviation path remained similar; however it exhibited greater lateral variation.

4.6 Estimation of Helicopter Fuselage Aerodynamic Data using CFD

The previous section demonstrates how aerodynamic properties of the slung load play a significant role in determining dynamic stability. At present, no complete set of fuselage aerodynamic data exists for any of the helicopters operated by the ADF. As part of the sustainment of DSTO's flight dynamic models, opportunity arose to model the MRH 90 and ARH fuselages using CFD. Results are shown for the MRH 90.

It is very difficult to accurately estimate load aerodynamic characteristics without a comprehensive aerodynamic analysis tool. This research aims to generate aerodynamic data for a range of bodies using open source CFD software.

Most commercial CFD software has the ability to model complex geometries such as helicopter fuselages. The advantage of open source CFD software is that the developer has full access to the underlying code, affording the ability to generate more tailored solutions.

OpenFoam was chosen to trial the feasibility of using open source software to analyse complex geometries. To test basic functionality, a two dimensional validation case for flow over a cylinder was performed. From this, drag coefficients were determined.

The geometry and mesh were created in the open source program Gmsh. The mesh was subsequently used with OpenFoam to produce aerodynamic data. For high Reynolds number flow, good agreement was obtained between experimental results of Zahm [11] and the OpenFoam predictions. This validation case was able to provide the process and procedures required to study more complex geometries.

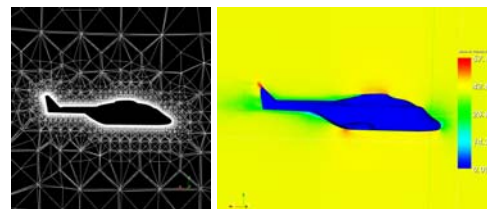


Figure 15 Mesh domain (left) and velocity field (right) at a representative operational airspeed of 80 knots for the MRH 90

A similar procedure was then employed for the three dimensional MRH 90 helicopter fuselage geometry. Initially, only the zero angle of attack onset flow

was considered. Fig. 15 shows the mesh domain generated and a representative velocity field. For further details see reference [4].

While flow cases for a number of angles of attack and for all flow directions have not yet been completed, progress has been made in improving understanding of the OpenFoam solver and a range of open source CFD tools. Additionally, the initial comparison between results generated in OpenFoam and those calculated using the commercial product Fluent show good agreement for integrated forces, surface pressure and wall shear stress.

5. CONCLUDING REMARKS

A simulation model has been developed using the equations of motion for general slung load systems. This model has been used to examine the effect of various parameters. This includes the investigation into the dynamic and aerodynamic parameters of slung loads, and the effects of load mass variation, cg location, helicopter speed, rigging configuration, load geometry and pilot control input magnitude on slung load stability.

The preliminary results of the research presented in this paper cover the nature of load oscillations and maximum load position deviations. It is hoped these results will aid operators in the identification of load parameters most critical to load stability.

From the test scenarios detailed, the following general conclusions can be drawn, although some contradictory conditions also exist.

- The lighter the load the greater the maximum load position deviation

- Increasing forward speed increases maximum load position deviation
- The load experiences increased stability for cg positions forward of the centre-point
- The larger the pilot control input magnitude, the larger the maximum load position deviation
- The influence of load orientation on aerodynamic behaviour must be considered
- Sling configuration has a significant effect on the nature of load position deviation
- Increasing CD and CL decreases maximum load position deviation

This research is expected to continue and simulation results that do not follow the general trends will be more closely examined. Development of open source CFD tools will also continue.

6. REFERENCES

- [1] Stuckey, R.A. (2001) Mathematical Modelling of Helicopter Slung-Load Systems, *DSTO Technical Report*, TR-1257.
- [2] Cicolani, L. S. and G. Kanning (1986), General equilibrium characteristics of a dual-lift helicopter system, NASA-TP-2615; A-86114; NAS 1.60:2615.
- [3] Boeing (2005), CH-47F Chinook, Product Information Book.
- [4] Burns, A., Vun, S., Blacker, N., Giacobello, M. and Reddy, R. (2008) Estimation of Helicopter Fuselage Aerodynamic Characteristics using CFD Tools, DSTO Technical Report, in preparation.

- [5] Stuckey, R. A (1998) Dynamic Simulation of the CH-47D Helicopter with Single and Multiple Loads, 2nd Australian-Pacific Vertiflite Conf. on Helicopter Technology, ADF Academy & AHS.
- [6] The MathWorks (1999) Inc., MATLAB, The Language of Technical Computing: Using Matlab Version 5 , The Mathworks, Natick, MA.
- [7] Heffley, R. (1997) ROTORGEN Minimal-Complexity Simulator MathModel with Application to Cargo Helicopters, NASA-CR-196705, HohAeronautics, Inc. CA.
- [8] Ronen, T. (1986) Dynamics of a Helicopter with a Sling Load, Ph.D. thesis, Stanford Univ., CA.
- [9] Hoerner, S. and H. Borst (1975) Fluid-Dynamic Lift, Hoerner Fluid Dynamics, Midland Park, NJ.
- [10] ESDU, (1980) Item No.80025: Mean Forces, Pressures and Flow Field Velocities for Circular Cylindrical Structures: Single Cylinder with Two-Dimensional Flow, Eng Sci Data Unit, UK.
- [11] Zahm, A.F. (1927). Flow and Drag Formulas for Simple Quadrics. NACA Annual Report. Vol 12, pg 515-537.